NANO LETTERS

2008
Vol. 8, No. 1
232−236

Noncovalent Functionalization of Carbon Nanotubes with Amphiphilic Gd^{3+} Chelates: Toward Powerful T_1 and T_2 MRI Contrast Agents

Cyrille Richard,*,† Bich-Thuy Doan,‡,§ Jean-Claude Beloeil,‡,§ Michel Bessodes,† Éva Tóth,§ and Daniel Scherman*,†

Unité de Pharmacologie Chimique et Génétique; CNRS, UMR 8151, Paris, F-75270 cedex France; Inserm, U 640, Paris, F-75270 cedex France; Université Paris Descartes, Faculté des Sciences Pharmaceutiques et Biologiques, Paris, F-75270 cedex France; ENSCP, Paris, F-75231 cedex France; Laboratoire de RMN Biologique, ICSN, CNRS, UPR 2301, 91198 Gif-sur-Yvette cedex France, and CBM, CNRS, UPR 4301, Rue Charles Sadron, 45071 Orléans cedex France

Received October 1, 2007

ABSTRACT

An amphiphilic gadolinium (III) chelate (GdL) was synthesized from commercially available stearic acid. Aqueous solutions of the complex at different concentrations (from 1 mM to 1 μM) were prepared and adsorbed on multiwalled carbon nanotubes. The resulting suspensions were stable for several days and have been characterized with regard to magnetic resonance imaging (MRI) contrast agent applications. Longitudinal water proton relaxivities, r_1, have been measured at 20, 300, and 500 MHz. The r_1 values show a strong dependence on the GdL concentration, particularly at low field. The relaxivities decrease with increasing field as it is predicted by the Solomon–Bloembergen–Morgan theory. Transverse water proton relaxation times, T_2, have also been measured and are practically independent of both the frequency and the GdL concentration. An in vivo feasibility MRI study has been performed at 300 MHz in mice. A negative contrast could be well observed after injection of a suspension of functionalized nanotubes into the muscle of the leg of the mouse.

Magnetic resonance imaging (MRI) is one of the most powerful diagnostic techniques in clinical medicine for in vivo assessment of anatomy and biological function.[1,2] MRI is based on the property of mainly water hydrogen nuclei to precess around an applied magnetic field. By applying radio frequency pulses and magnetic field gradients, the relaxation processes through which they return to their original aligned state can be exploited to give an image. The contrast of the image is related to various physical parameters, such as the local differences in spin relaxation kinetics along the longitudinal (spin−lattice relaxation time, T_1) and transverse (spin−spin relaxation time, T_2) planes of the main magnetic field applied to the specimen. Paramagnetic contrast agents (CA) are frequently used to enhance the image contrast.[3] They reduce T_1 (positive agents) and/or T_2 (negative agents) relaxation times of water protons. Positive contrast agents are Gd^{3+} complexes in majority and provide brighter images, whereas negative contrast agents are mainly superparamagnetic iron-oxide nanoparticles and produce darker images.[4] The efficiency of an MRI CA is expressed in terms of its relaxivity ($r_{1,2}$), defined as the paramagnetic relaxation rate enhancement referred to 1 mM concentration of the agent.[5] The clinically used Gd^{3+} complexes have low relaxivities. To increase their efficacy, the number of Gd^{3+} ions should be increased. Relaxivity is strongly dependent on the molecular motion, hence on the size and rigidity of the Gd^{3+} chelate. In the recent years, various macromolecular carriers have been explored, involving proteins,[6] dendrimers,[7] linear polymers,[8] water-soluble fullerenes,[9] or micellar structures.[10]

Carbon nanotubes are ultrasmall cylinders of few micrometers in length and several nanometers in diameter, exclusively made of carbon atoms.[11] Recently, we have reported the noncovalent functionalization of carbon nanotubes via chemical adsorption of various anionic surfactants.[12] The negative charge created by the surfactant adsorbed on the nanotube surface prevents their aggregation and induces stable suspensions in water. We report herein the first example of noncovalent functionalization of the outer surface

* Corresponding authors. E-mail: (C.R.) cyrille.richard@univ-paris5.fr.
† Unité de Pharmacologie Chimique et Génétique; CNRS, UMR 8151, Paris, F-75270 cedex France; Inserm, U 640, Paris, F-75270 cedex France; Université Paris Descartes, Faculté des Sciences Pharmaceutiques et Biologiques, Paris, F-75270 cedex France; ENSCP, Paris, F-75231 cedex France.
‡ Laboratoire de RMN Biologique, ICSN, CNRS, UPR 2301, 91198 Gif-sur-Yvette cedex France.
§ CBM, CNRS, UPR 4301, Rue Charles Sadron, 45071 Orléans cedex France.

10.1021/nl072509z CCC: $40.75
Published on Web 12/19/2007

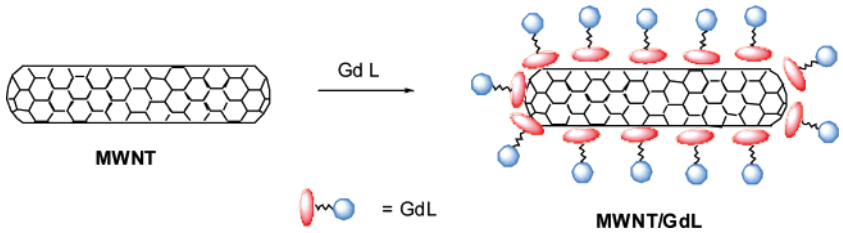

Figure 1. Carbon nanotubes noncovalently functionalized by amphiphilic Gd^{3+} chelates.

Scheme 1. Synthesis of the Amphiphilic H_5L from Stearic Acid.

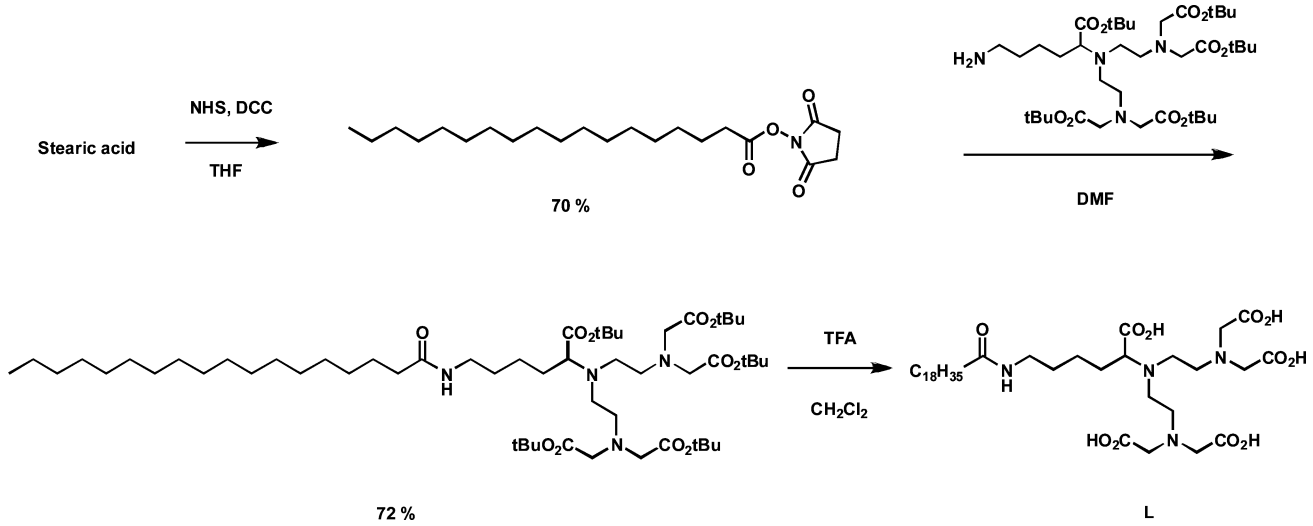

of carbon nanotubes by amphiphilic Gd^{3+} chelates and their effect on water proton relaxation in vitro and in vivo. The reagent (L) synthesized in this work is composed of (i) a lipid chain capable of surface adsorption on the nanotubes via van der Waals interactions and (ii) a $DTPA^{5-}$ polar head to suspend multiwalled carbon nanotubes (MWNT) in aqueous solution and chelate Gd^{3+} (Figure 1). This system is water compatible, Gd^{3+} ions are complexed to a strong chelator (DTPA) preventing toxicity concerns, and they are present on the entire surface of the nanotubes (and not only around side-wall defects)[13] making it directly accessible to water molecules and easily adjustable.

The bifunctional reagent L was prepared in three steps[14] from commercially available stearic acid (Scheme 1) and a DTPA-derivative[15] (see Supporting Information). Solutions of GdL (0.8 equiv of Gd^{3+} per L) at different concentrations (from 1 mM to 1 μM) were prepared in water at pH 7.8 using $GdCl_3$. One mL of each solution was added to 1 mg of MWNT (Aldrich, 0.5−2 μm in length) and sonicated for 3 min to obtain suspensions. Solutions of MWNT/GdL at GdL concentrations <0.05 mM were found to be less stable; therefore, they were not further investigated. This result is in accordance with previous observations that showed that the presence of micelles is a key step for the formation of stable supramolecular assemblies on the nanotube surface.[11] For an amphiphilic Gd^{3+} chelate bearing a C_{18} hydrophobic chain, a critical micelle concentration (cmc) of 0.06 mM has been reported,[16] and we can expect a value in the same range for GdL. Concentrations around and above the cmc seem to be required for the surfactant to keep the nanotubes in suspension. For MWNT/GdL solutions of ≥0.05 mM GdL concentration, longitudinal and transverse relaxation rates were measured with inversion recovery and Carr−Purcell−Meiboom−Gill (CPMG) techniques, respectively, at proton Larmor frequencies of 20 MHz (Bruker Minispec), 300 MHz (Varian NMR spectrometer Inova, Palo Alto, CA and Bruker Biospec spectrometer, Wissembourg, France), and 500 MHz (Bruker Avance NMR spectrometer, Wissembourg, France) and 25 °C. The relaxation rate measurements were reproducible with independent samples.

The longitudinal proton relaxivities, r_1, measured at the different GdL concentrations and frequencies are presented in Figure 2. The relaxities are calculated according to $r_1 = (1/T_{1obs} - 1/T_{1dia})/C_{Gd}$, where $1/T_{1obs}$ and $1/T_{1dia}$ are the observed and the diamagnetic relaxation rates, and C_{Gd} is the concentration of GdL in mM. The r_1 values show a strong dependence on the GdL concentration, particularly at low field. The relaxivities decrease with increasing field as it is predicted by the Solomon−Bloembergen−Morgan theory of paramagnetic relaxation.[2] This decrease becomes more important as the concentration of GdL is decreasing, which indicates that the rotational motion becomes slower with decreasing GdL concentration. It should be noted that the nanotubes solubilized with L but without Gd^{3+} have no detectable influence on the longitudinal relaxation of water protons. We can rationalize these observations in terms of an aggregation phenomenon. This aggregation is more significant in solutions with lower GdL concentration where there are not enough negatively charged complexes adsorbed on the nanotube surface to efficiently prevent aggregation.

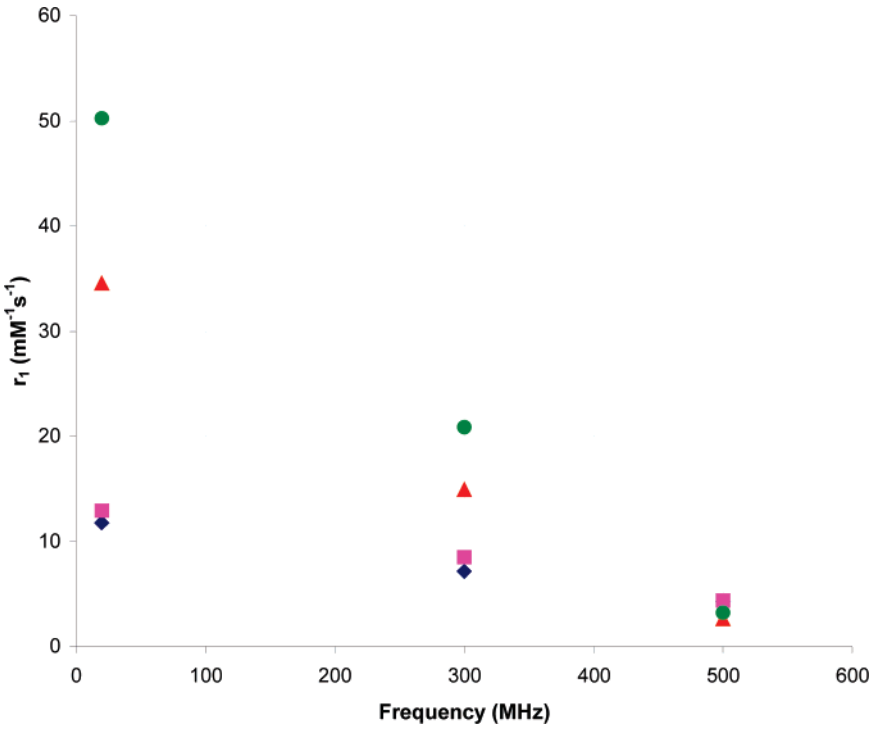

Figure 2. Longitudinal proton relaxivities of MWNT/GdL solutions at GdL concentrations of 1.0 (diamonds), 0.5 (squares), 0.1 (triangles), and 0.05 mM (circles), 25 °C.

Similar aggregation phenomena were previously proved to exist in aqueous solutions of water soluble gadofullerenes and were responsible for their elevated relaxivities.[17]

The proton relaxivities are particularly high at 20 MHz with 0.1 and 0.05 mM GdL concentrations: 34.5 and 50.3 mM^{-1} s^{-1}, respectively, in comparison to 4.7 $mM^{-1}s^{-1}$ for GdDTPA (Magnevist), a clinically used Gd^{3+}-based contrast agent under the same conditions. On the other hand, the r_1 values measured at 0.5 and 1.0 mM GdL concentrations at 20 MHz are relatively low (12.9 and 11.8 mM^{-1} s^{-1}). The low r_1 values seem to indicate that the flexibility of the polar head containing the Gd^{3+} is very important for these systems and seriously limits the relaxivities. It is interesting to note that for an amphiphilic chelate also with a C_{18} chain that forms micelles in aqueous solution, a relaxivity of 20.8 mM^{-1} s^{-1} was measured at 20 MHz and 25 °C.[16] A similar value could be expected for a micellar solution of GdL without MWNT. The different relaxivity observed for GdL in the presence of the nanotubes proves that the GdL complexes are not present in the form of micelles but they are indeed adsorbed on the nanotubes. Unfortunately, the effective motion of the Gd^{3+} chelates in these structures seems to be much faster than in the micelles, which results in the lower relaxivity.

Transverse relaxation times, T_2, have also been measured on these samples at three different proton Larmor frequencies: 20, 300, and 500 MHz (Table 1). The T_2 values at all frequencies and any GdL concentrations are remarkably lower than that of pure water, and they are practically independent of both the frequency and the GdL concentration (8.5−13.8 ms for MWNT/GdL versus 2500 ms for water).

Table 1. Transverse Relaxation Times (T_2, ms) of MWNT/GdL at Different Frequencies and GdL Concentrations

	Frequency		
[GdL]	20 MHz	300 MHz	500 MHz
1 mM	13.8 ms	8.5 ms	10.8 ms
0.5 mM	13.4 ms	9.8 ms	12.0 ms
0.1 mM	11.4 ms	8.8 ms	13.7 ms
0.05 mM	12.7 ms	9.8 ms	13.5 ms

Table 2. Transverse Relaxation Times (T_2, ms) of MWNT/L at 300 MHz and Different L Concentrations

	Frequency
[L]	300 MHz
1 mM	13.7 ms
0.5 mM	16.5 ms
0.1 mM	21.2 ms
0.05 mM	12.4 ms

These results led us to measure the transverse relaxation times T_2 of suspensions containing MWNT and the amphiphilic ligand L at various concentrations without any Gd^{3+}. The values obtained were in the same range as those measured in the solutions containing Gd^{3+} (Table 2).

Consequently, the T_2 effect is exclusively related to the presence of the suspension of carbon nanotubes and independent of Gd^{3+}. Carbon nanotubes can be viewed as giant conjugated molecular wires with a conjugation length corresponding to the length of the tube that create strong inhomogeneities and potential magnetic susceptibility effects.[18] The electronic states of a carbon nanotube form one-dimensional electron and hole sub-bands, separated by an

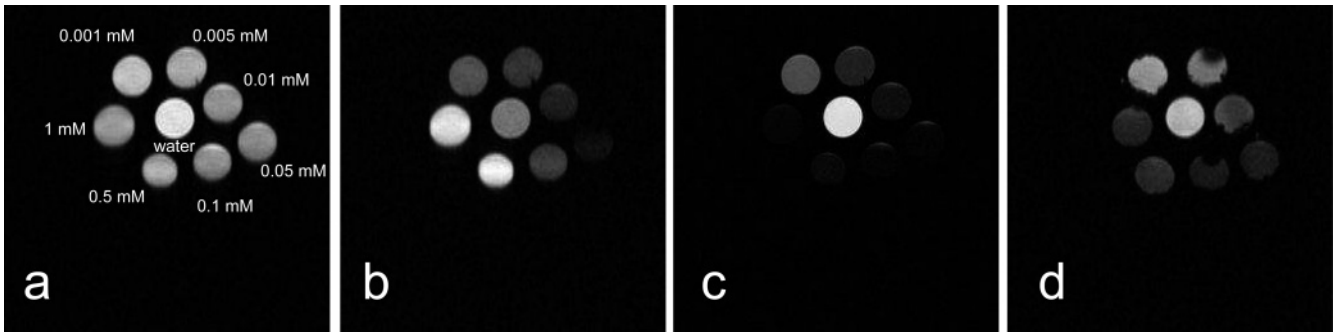

Figure 3. MRI images of the MWNT/GdL complex with different weightings and concentrations measured at 300 MHz. (a) Rho-weighted SE TR/TE = 15 s/10 ms, (b) T_1-weighted SE TR/IR/TE = 15 s/1 s/10 ms with hypersignal for the Gd concentrated complex, (c) T_2-weighted SE TR/TE = 15 s/33 ms with hyposignal for the concentrated Gd complex, and (d) T_2*-weighted with relative signal intensity as panel c GE TR/TE = 15 s/9 ms, FOV = 5 cm, final 256 × 256 matrix resolution.

Figure 4. T_2*-weighted gradient echo sequence with breath triggering. Coronal in vivo MR image of the muscle of the mouse legs after MWNT/L injection (left leg, white arrow) and lipid L injection (right leg, black arrow).

energy gap. States near the energy gap are predicted to have an orbital magnetic moment, which is much more significant than the Bohr magneton. This magnetic moment, generated by the motion of electrons around the circumference of the tube, was proposed to be the origin of the magnetic susceptibility of carbon nanotubes.[18,19] In fact, carbon nanotubes have a significantly larger orientation-averaged susceptibility on a per carbon basis than any other form of elemental carbon.[20] The important T_2 effect observed in the nanotube solutions can be likely related to these phenomena. However, the exact mechanisms involved are not explored yet, and gaining such a mechanistic insight is far beyond the scope of the present study.

In the objective of assessing the potential of this nanotube/GdL assembly with respect to an application as T_1 and/or T_2 MRI contrast agent, in vitro MRI experiments were recorded on proton density, T_1, T_2, and T_2* weighted contrast at 300 MHz on an MRI spectrometer. Figure 3a displays a reference proton density image, where all MWNT/GdL samples and the water reference sample have a high-intensity signal. In the T_1-weighted image, the nanotube samples containing higher GdL concentration are in hypersignal compared to the water reference sample (Figure 3b). On the other hand, in the T_2- and T_2*-weighted images (Figure 3c,d, respectively) the tubes with higher GdL concentrations appear in hyposignal, as predicted by the T_1 and T_2 values previously measured. T_2* values were too small to be quantified (suggesting a short value inferior to 5−10 ms). Clearly, the T_2 and T_2* effects are predominant as compared to the T_1 effect. A sufficient T_1 contrast would require considerably high GdL concentrations (here >0.1 mM in vitro). Consequently, T_2 weighting was privileged for further in vivo experiments.

To evaluate the efficiency of this novel system for in vivo applications, preliminary experiments were performed by injecting 50 μL of the less concentrated suspension (MWNT/L

at L concentration of 0.05 mM) into the muscle of the leg of anesthetized mouse (BALB/c, 25 g, male, Janvier, France). Five mice were intramuscularly injected. MRI studies were performed in agreement with the French guidelines for animal care. As it is clearly visible in Figure 4, a negative contrast is easily detected as a dark area (white arrow) at the site of injection. When 50 μL of a solution of the lipid L alone (at identical concentration as above, but without nanotubes) were injected, no contrast appeared (black arrow). Similar results were obtained if a suspension of MWNT/L was injected in the liver (image not shown). These nanomaterials were well tolerated by the mice. No apparent side effects were observed during the injection, immediately or days after the experiment. Indeed, 100% survival of the animals was obtained after more than 1 month.

In summary, we report the first example of carbon nanotubes noncovalently functionalized by amphiphilic GdL chelates as potential MRI contrast agents. The functionalized nanotubes proved to be simultaneously powerful positive and negative CA. Experiments are in progress to evaluate the influence of parameters like the concentration and the nature of carbon nanotubes on the T_1 and T_2 relaxation times. Furthermore, their use as potential contrast agent for in vivo applications is also under investigations.

Acknowledgment. This paper is dedicated to the memory of Dr. Charles Mioskowski, deceased on June 2, 2007. We are grateful to Dr. Pierre Smirnov for his help in some of the relaxivity measurements. We thank the CNRS-CEA "Imagerie du Petit Animal" and EMIL project for financial support (European-funded EMIL programme LHSC−2004 503569). This work was performed in the frame of the EU COST Action D38 "Metal-Based systems for Molecular Imaging Applications".

Supporting Information Available: Experimental details for the synthesis of L. This material is available free of charge via the Internet at http://pubs.acs.org.

References

(1) Caravan, P.; Ellison, J. J.; McMurry, T. J.; Lauffer, R. B. *Chem. Rev.* **1999**, *99*, 2293−2352.
(2) Merbach, A. E.; Toth, E. *The Chemistry of Contrast Agents in Medical Magnetic Resonance Imaging*; John Wiley & Sons: New York, 2001.
(3) Tilcock, C. *Adv. Drug Delivery Rev.* **1999**, *37*, 33−51.
(4) Weissleder, R.; Papisov, M. *Rev. Magn. Reson. Med.* **1992**, *4*, 1−20.
(5) Aime, S.; Botta, M.; Fasano, M.; Terreno, E. *Chem. Soc. Rev.* **1998**, *27*, 19−29.
(6) Lauffer, R. B.; Parmelee, D. J.; Dunham, S. U.; Ouellet, H. S.; Dolan, R. P.; Witte, S.; McMurry, T. J.; Walovitch, R. C. *Radiology* **1998**, *207*, 529−538.
(7) Wiener, E. C.; Brechbiel, M. W.; Brothers, H.; Magin, R. L.; Gansow, O. A.; Tomalia, D. A.; Lauterbur, P. C. *Magn. Res. Med.* **1994**, *3*, 1−8.
(8) Aime, S.; Botta, M.; Frullano, L.; Garino, E.; Crich, S. G.; Giovenzana, G. B.; Pagliarin, R.; Palmisano, G.; Sisti, M. *Chem.−Eur. J.* **2000**, *6*, 2609−2619.
(9) Toth, E.; Bolskar, R. D.; Borel, A.; Gonzalez, G.; Helm, L.; Merbach, A. E.; Sitharaman, B.; Wilson, L. J. *J. Am. Chem. Soc.* **2005**, *127*, 799−805.
(10) Accardo, A.; Tesauro, D.; Roscigno, P.; Gianolio, E.; Paduano, L.; D'Errico, G.; Pedone, C.; Morelli, G. *J. Am. Chem. Soc.* **2004**, *126*, 3097−3107.
(11) Iijima, S. *Nature* **1991**, *354*, 56−58.
(12) Richard, C.; Balavoine, F.; Schultz, P.; Ebbesen, T. W.; Mioskowski, C. *Science* **2003**, *300*, 775−778.
(13) Sitharaman, B.; Kissell, K. R.; Hartman, K. B.; Tran, L. A.; Baikalov, A.; Rusakova, I.; Sun, Y.; Khant, H. A.; Ludtke, S. J.; Chiu, W.; Laus, S.; Toth, E.; Helm, L.; Merbach, A. E.; Wilson, L. J. *Chem. Commun.* **2005**, *31*, 3915−3917.
(14) Mignet, N.; le Masne de Chermont, Q.; Randrianarivelo, T.; Seguin, J.; Richard, C.; Bessodes, M.; Scherman, D. *Eur. Biophys. J.* **2006**, *35*, 155−161.
(15) Anelli, P. L.; Fedeli, F.; Gazzotti, O.; Lattuada, L.; Lux, G.; Rebasti, F. *Bioconjugate Chem.* **1999**, *10*, 137−170.
(16) Nicolle, G. M.; Tóth, E.; Eisenwiener, K.-P.; Mäcke, H. R.; Merbach, A E. *J. Biol. Inorg. Chem.* **2002**, *7*, 757−769.
(17) Laus, S.; Sitharaman, B.; Tóth, E.; Bolskar, R. D.; Helm, L.; Asokan, S.; Wong, M. S.; Wilson, L. J.; Merbach, A. E. *J. Am. Chem. Soc.* **2005**, *127*, 9368−9369.
(18) Minot, E. D.; Yaish, Y.; Sazonova, V.; McEuen, P. L. *Nature* **2004**, *428*, 536−539.
(19) Glenis S.; Likodimos V.; Guskos N.; Lin C. L. *J. Magn. Magn. Mater.* **2004**, *272−276*, 1660−1661.
(20) Ramirez, A. P.; Haddon, R. C.; Zhou, O.; Feming, R/M.; Zhang, J.; McClure, S. M.; Smalley, R. E. *Science* **1994**, *265*, 84−86.

NL072509Z